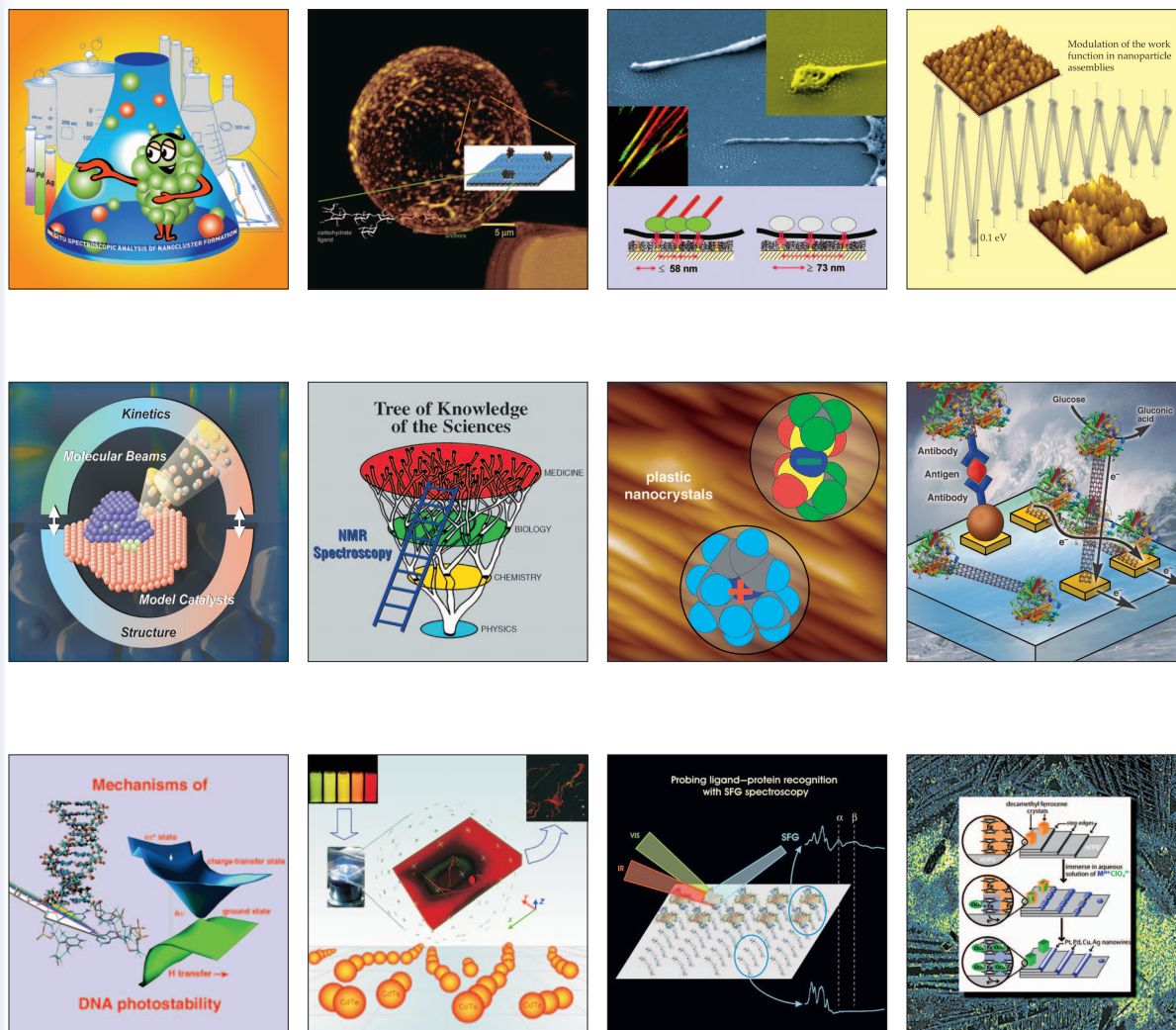


A EUROPEAN JOURNAL

CHEMPHYSICHEM

OF CHEMICAL PHYSICS AND PHYSICAL CHEMISTRY



Reprint

© Wiley-VCH Verlag GmbH & Co. KGaA, Weinheim

 WILEY-VCH

A EUROPEAN JOURNAL

CHEMPHYSICHEM

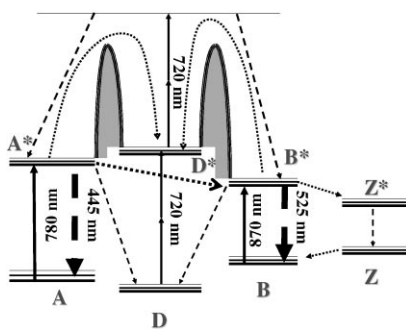
OF CHEMICAL PHYSICS AND PHYSICAL CHEMISTRY

Table of Contents

G. Chirico,* A. Diaspro, F. Cannone,
M. Collini, S. Bologna, V. Pellegrini,
F. Beltram

328 – 335

**Selective Fluorescence Recovery after
Bleaching of Single E²GFP Proteins
Induced by Two-Photon Excitation**



Permanently blinking proteins: Fluorescence recovery of the green fluorescent protein (GFP) mutant E²GFP can be obtained with high efficiency by laser irradiation in the near infrared, at 720 nm (see scheme of the electronic level structure). This GFP mutant seems promising as an “almost permanent” chromophore for two-photon excitation microscopy or for applications in single-molecule memory arrays.

Selective Fluorescence Recovery after Bleaching of Single E²GFP Proteins Induced by Two-Photon Excitation**

G. Chirico,^{*[a]} A. Diaspro,^[c] F. Cannone,^[a] M. Collini,^[a] S. Bologna,^[d] V. Pellegrini,^[b] and F. Beltram^[b]

We report the two-photon excitation and emission of a recently developed green fluorescent protein (GFP) mutant, E²GFP. Two main excitation bands are found at 780 and 870 nm. Blinking and irreversible and reversible bleaching were observed. Fluorescence blinking occurs in the millisecond range and has been ascribed to conversions between the neutral, anionic and dark zwitterionic states. Bleaching is observed after approximately 10 to

4000 ms depending on the excitation power, and it is probably due to a conversion to a dark state. The striking feature of this GFP mutant is that the fluorescence can be recovered with very high efficiency only upon irradiation at 720 ± 10 nm. This GFP mutant therefore seems promising as an almost permanent chromophore for two-photon excitation (TPE) microscopy or for applications in single-molecule memory arrays.

Introduction

Fluorophores display photobleaching, a permanent and irreversible loss of fluorescence emission.^[1,2] This process limits the observation time of fluorescence emission from biological samples, especially when high excitation intensities are used, as in confocal and two-photon microscopy.^[3,4] Most of the chromophores for biological applications have also pronounced blinking in the microsecond-to-millisecond range.^[5,6] Bleaching should be taken carefully into account in the application of fluorescence microscopy to the study of long-lasting cellular processes at high spatial resolution. The control of the chromophore emission is therefore an essential step for a wider and more effective application of fluorescence microspectroscopy to cellular environments. In this framework, some biological systems, such as the green fluorescent protein (GFP) of the *Aequorea Victoria* jellyfish, offer naturally evolved optimized structures with unique properties that can be further tailored to specific applications by genetic engineering.^[7,8,9] GFP has emerged in recent years as a unique fluorescent marker in molecular and cell biology.^[10,11] GFP fluorescence dynamics are characterized by transitions between bright and dark states which, at the single-molecule level, lead to reversible turning on and off (blinking) of the emission.^[5,6,12] Blinking of GFP mutants has been addressed in a number of works mainly by single-molecule techniques.^[13] Photobleaching of GFP mutants^[14,15,16] and different types of photoactivation processes have also been reported and studied. Dickson et al.^[12] were able to recover fluorescence emission from apparently irreversibly photobleached YFP molecules (that carry the T203Y mutation) with 405-nm irradiation. On the other hand, Cinelli et al.^[15] have demonstrated no optical switching behavior for EGFP under a variety of conditions, while spontaneous recovery of fluorescence has been reported for GFP mutants carrying the E222Q mutation. Jung et al.^[17] found recovery times as long as 180 min after bleaching, and these results have been

confirmed and extended by Garcia-Parajo et al.^[6] on the S65T mutant of GFP. More recently Jung et al.^[18] have demonstrated the photoinduced enhancement in the fluorescence output of a E222Q-GFP mutant by dual color excitation. Recently Lippincott-Schwartz and Patterson^[14] gave an overview of three different protein mutants, PA-GFP,^[19] Kaede^[20] and KFP1^[21] that represent a choice as photoactivated fluorescent proteins. PA-GFP^[19] is the only GFP mutant of these series, and it is characterized by a mutation at the threonine 203 (T203H).

Herein, we report the two-photon excitation (TPE) of fluorescence of single molecules of E²GFP, a recently developed GFP mutant,^[22] in terms of the quantum yields, cross sections, lifetimes, and dependence upon pH. E²GFP is a triple mutation of GFP (F64L, S65T, T203Y) obtained by a T203Y mutation of EGFP.^[15,22] The main result of this study is the finding that fluorescence is recovered after photobleaching only upon selective irradiation with near-infrared (IR) light. The fluorescence recovery is highly efficient and its dependence upon the irradiation wavelength is very sharp. These features offer the possibility to

[a] Prof. G. Chirico, Dr. F. Cannone, Dr. M. Collini
INFN and Department of Physics, University of Milano Bicocca
Piazza della Scienza 3, 20126 Milano (Italy)
Fax: (+39) 2-644-82894
E-mail: giberto.chirico@mib.infn.it

[b] Dr. V. Pellegrini, Prof. F. Beltram
NEST-INFN and Scuola Normale Superiore
Piazza dei Cavalieri 7, 56126 Pisa (Italy)

[c] Prof. A. Diaspro
INFN and Department of Physics, University of Genoa
Via Dodecaneso 33, 16146 Genova (Italy)

[d] Dr. S. Bologna
Department of Biochemistry and Molecular Biology
University of Parma, 43100 Parma (Italy)

[**] E²GFP = green fluorescent protein mutant

use E²GFP for intracellular studies of slow biological processes by means of single-molecule two-photon excitation.

Experimental Section

Optical Setup: The optical setup is built around an inverted microscope (TE300, Nikon, Japan) with a Plan Apochromat 100X oil objective (N.A.=1.4, Nikon, Japan) and a PCM2000 Nikon scanning head coupled to a femtosecond mode-locked Ti:sapphire laser (Tsunami 3960, Spectra Physics, CA) as described elsewhere.^[23] The fluorescence signal, collected by an objective and spectrally resolved by either emission filters (HQ535/30=535±15 nm, HQ440/50=440±25 nm and SP670=short pass at 670 nm, Chroma Inc., Brattleboro, VT) or a Jobin-Ivon monochromator, is fed to a multi-mode fiber that brings the light to a photomultiplier (R928, Hamamatsu, Milano, Italy) in the PCM2000 controller.^[23] The point spread function widths of the setup measured at $\lambda=740$ nm are 220 ± 40 nm in the radial direction and 790 ± 50 nm in the axial direction (statistical accuracy means standard deviation herein).^[24]

Sample Preparation: E²GFP is a triple mutation (F64 L, S65T, T203Y) obtained as a mutation of EGFP (F64 L, S65T). E²GFP has been prepared as a recombinant protein, as described by Cinelli et al.^[15] For single-molecule studies, the E²GFP molecules were encapsulated in silica gels.^[25] We have shown previously^[26] that this trapping matrix allows protein rotational motions and does not change the main chemical and physical properties of the protein. The stock protein solution was diluted 50- to 100-fold in citrate buffer (10 mM citrate, 100 mM phosphate buffer, pH 5.0). The final solution was mixed with the solution (in a 7:10 ratio), obtained with tetramethyl-orthosilicate, water, hydrochloric acid, and phosphate buffer. Silica gels were then covered with the same buffer solution and stored at 4°C for at least 12 h before use. The gel pore size is estimated to be less than a few nanometers and the E²GFP molecules, which have an average diameter of about 4 nm, were not observed to leak through the gels. The E²GFP concentration in silica gel is estimated around 10 nM. All experiments were performed at room temperature.

Fluorescence Imaging: The images (512×512 pixels) of encapsulated fluorescent proteins were acquired with a residence time of 3 μ s per pixel, a field of view $\approx 10\ \mu\text{m}\times 10\ \mu\text{m}$ and excitation power $\approx 3\text{--}15$ mW on the sample. The single-molecule spot corresponds to approximately 11×11 pixels for this choice of imaging parameters. The effective collection time of fluorescence per single protein is therefore $\approx 360\ \mu\text{s}$. The single proteins were not irradiat-

ed during the rest of the image acquisition. The images typically showed several distinct spots ascribed to the fluorescence signal from either single proteins or small aggregates. Single-molecule spots were then identified according to a histogram analysis of the fluorescence output, as described elsewhere^[27] and to the observation of a sudden single-step bleaching on our sampling time scale ($\approx 360\ \mu\text{s}$).

Fluorescence Spectra Acquisition: The fluorescence emission spectrum was acquired through a monochromator (Jobin-Yvon, Longjumeau, France, model H10-450) with a 4 nm spectral resolution. Fluorescence excitation spectra were obtained on aggregates of ≈ 10 E²GFP molecules encapsulated in silica gel, and by varying the excitation wavelength (700–920 nm) at fixed excitation power on the sample (1 mW), or by collecting the fluorescent signal through various emission filters (SP670, and HQ440/50 and HQ535/30). The emission and excitation spectra shown in the Figure 1 are the average of the spectra taken on ≈ 10 aggregates.

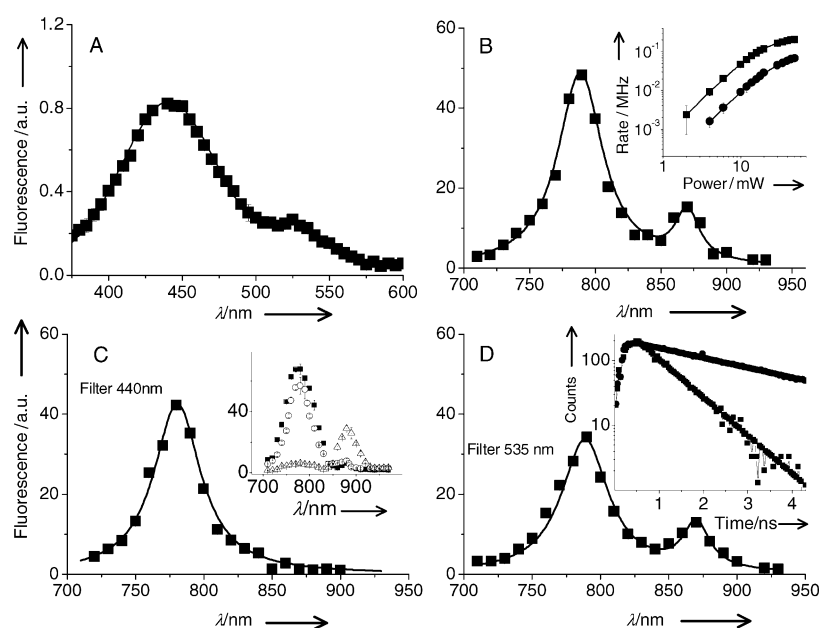


Figure 1. Panel A: two-photon fluorescence emission spectrum upon excitation at $\lambda=760$ nm at constant excitation power (1 mW, silica gel pH 5). Panels B, C and D: two-photon fluorescence excitation spectra of E²GFP trapped in silica gels (≈ 10 molecules/excitation volume). The solid lines are best fits to the sum of two Lorentzians. Panel B reports the fluorescence emission observed through a short-pass IR filter (< 670 nm). Panels C and D report the fluorescence emission observed through 440/50 and 535/30 emission filters. Inset of panel B: fluorescence emission averaged over ≈ 100 single molecules for the A state (■) with excitation at 780 nm and emission through the 440/50 filter (transmission $\approx 94\%$), and for the state B (●) with excitation at 870 nm and emission through the 535/30 filter (transmission $\approx 60\%$). The data have been computed by summing all the photons collected on a single-protein spot, which corresponds to ≈ 120 pixels, and for a total of 360 μs illumination time of the single protein. Solid lines are the best fits to the function: $\alpha P^2/[1 + (P/P_{\text{saturation}})^2]$. The best-fit values are reported in the text. Inset of panel C: fluorescence excitation spectra taken on small protein aggregates in the gels and observed through the short-pass emission filter at pH 5.8 (■), 7.4 (○) and 9 (△). Inset of panel D: fluorescence decay averaged over 100 molecules for the A (■) and B (●) states. The best-fit values are reported in the text.

Fluorescence Kinetics of Individual Spots: To study the E²GFP photodynamics, we collected sequential images for a total time of ≈ 10 s. The single-molecule illumination time in a 160×160 pixels image, is $\approx 360\ \mu\text{s}$. This corresponds to the illumination time per single protein on the image. Single proteins were not irradiated for the rest of the image acquisition, which lasted ≈ 229 ms. The stability of the microscope stage in the z direction was assessed as described previously.^[28]

Lifetime Measurements: We measured excited-state lifetime by means of a PCI board for time-correlated single photon counting (TCSPC) (Time Harp 200, PicoQuant, Berlin) connected to an Avalanche photodiode (APD; EG&G, Canada, I; model SPCM-AQR15) directly coupled to one of the bottom ports of the Nikon microscope. The lifetime measurement duration was less than the bleaching time, typically 4 s at 0.5 mW, and the temperature T was kept at 293 K in order to minimize the blinking and photoconversion probability. We verified that, on each acquisition run, no blinking event was detected. Each lifetime decay was obtained by counting typically 7000–15000 photons per single molecule.

Results

Excitation and Emission Spectra

TPE spectra of single E²GFP molecules are reported in Figure 1. The emission spectrum upon two-photon excitation at $\lambda \approx 780$ nm, shows two components at $\lambda \approx 445$ nm and at $\lambda \approx 525$ nm (Figure 1, panel A) and it is very similar in shape to the one-photon excitation (OPE) spectrum.^[22] The TPE spectra of single E²GFP molecules in silica gel, very similar to those in solution, have been acquired through three emission filters in order to select the full emission (SP670), the emission at 445 nm (HQ440/50) or the emission at 527 nm (HQ535/30). When the fluorescence is collected through the short-pass filter, two excitation bands at $\lambda = 780$ nm and $\lambda = 870$ nm are found (Figure 1, panel B) similar to the spectrum collected through the HQ535/30 filter (Figure 1, panel D). On the contrary, the excitation spectrum shows a single band ($\lambda = 780$ nm) when collected through the HQ440/50 filter (Figure 1, panel C). By comparing the two-photon emission and excitation spectra we suggest that the E²GFP mutant shows at least two TPE fluorescent states: state A ($\lambda_{\text{exc}} = 780$ nm, $\lambda_{\text{em}} = 445$ nm) and state B ($\lambda_{\text{exc}} = 870$ nm, $\lambda_{\text{em}} = 525$ nm). Moreover, we identify the states A and B as the neutral and anionic states of the chromophore. This assignment is further confirmed by the following considerations. When we increase the pH in the silica gel, we observe a decrease of the A band and a corresponding increase of the B band (Figure 1, panel C, inset). The fluorescence lifetime of E²GFP, measured on single proteins on the A (excitation at 780 nm, emission through the HQ440/50 filter) and B (excitation at 870 nm, emission through the HQ535/30 filter) channels, can be fitted to a single exponential decay for lag times > 300 ps (Figure 1, panel D, inset), finding lifetimes values of ≈ 1 ns and ≈ 2.8 ns, respectively. When we excite bulk solutions of E²GFP on either the neutral or the anionic channel we obtain a single exponential decay (for lag times larger than 0.3 ns) with values $\tau = 1.0 \pm 0.2$ ns and $\tau = 3.1 \pm 0.2$ ns, respectively. These are also the typical values of the lifetimes reported in the literature for the neutral and the anionic states of most of the GFP mutants.^[29] We notice here that Lossau et al., who have studied in detail the fluorescence decay of GFP mutants in the subnanosecond time window, report more than one lifetime component for the neutral state, with an average value ≈ 0.9 ns, in good agreement with our measurements. It is likely that we cannot resolve more than

one lifetime component in our measurements due to the time resolution of our setup.

Finally it is worth noting that the emission at $\lambda \approx 445$ nm could not be observed in ref. [22] only because a single-photon excitation at 476 nm was used. An excitation at 400 nm would probably have shown an emission at ≈ 445 nm. As a matter of fact the GFP blue-edge emission (here 445 nm) has been observed only once^[30,31] apart from the present data, and can be ascribed to a direct emission of the neutral state.

TPE Fluorescence Emission versus Excitation Power

We studied the fluorescence of more than 100 single E²GFP molecules at different excitation powers. The fluorescence emission versus the excitation power at 780 nm and 870 nm, in the range 0–15 mW, follows a second-order power law (Figure 1, panel B, inset). A saturation effect is evident for excitation powers larger than 10–15 mW for both states and is well accounted for^[4] by the function $\alpha P^2/[1 + (P/P_{\text{saturation}})^2]$. We find $\alpha_A = 0.6 \pm 0.02$ kHz m⁻¹ W⁻², $P_{\text{saturation}} = 20 \pm 0.8$ mW for state A, and $\alpha_B = 0.1 \pm 0.04$ kHz m⁻¹ W⁻², $P_{\text{saturation}} = 30 \pm 1$ mW for the state B.

Ground-State Population

When the same field of view is observed first in the A and then in the B channel, different single molecules are detected (Figure 2). We never observed a single protein spot on both channels. In order to check that no photobleaching effect is present we acquired a third image on the A channel and this always gave the same single-molecule spots observed in the image previously taken on the A channel. At acidic pH, the number $N(780,440)$ of single E²GFP observed in the A channel was always larger than that observed in the B channel, $N(870,535)$. The ratio $N(780,440)/N(870,535)$ depends on the pH (see the sequence of images and left graph in Figure 2). In fact when increasing the pH, we observe an increase of $N(870,535)$ and a decrease of $N(780,440)$, that is, at basic pH the B state is more populated than A state. The spots not enclosed in rectangles are aggregates (between four and seven proteins per aggregate) and clusters of aggregates. Their intensity decreases with pH when observed on the A channel but increases with pH when observed on the B channel. This trend reflects the change in the number of proteins on each channel per aggregate, in agreement with the observations done on the single-protein spots.

It is remarkable that we never observed the same molecule on both channels, neutral and anionic. This implies the existence of two stable and spectrally distinct species, the neutral and the anionic one, and highlights the strength of single-molecule spectroscopy in studying the molecular heterogeneity.

Single-Molecule Fluorescence Kinetics

Tens to hundreds of images of single E²GFP molecules could be recorded in the IR region 770–890 nm before the fluorescence dropped suddenly (i.e., within 360 μ s) to the back-

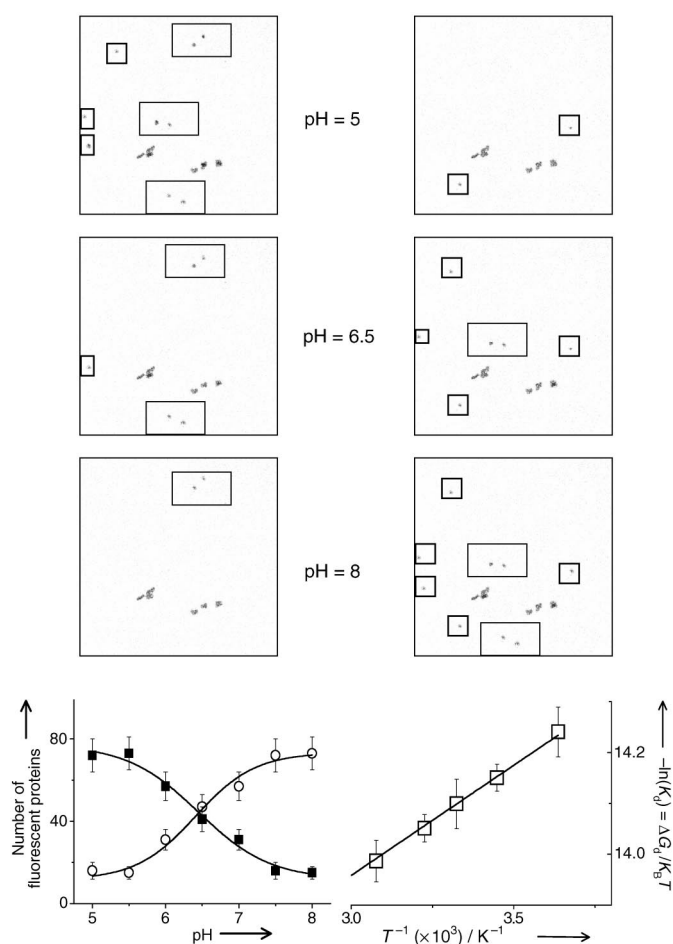


Figure 2. Fluorescence images of the same field of view, $10\ \mu\text{m} \times 10\ \mu\text{m}$ (512×512 pixels, $3\ \mu\text{s}$ dwell time, $10\ \text{mW}$ excitation power) through the A and B channels at different silica gel pH values. Left column: A channel (neutral state, excitation at $\lambda_{\text{exc}} = 780\ \text{nm}$ and collection through a 440/50 emission filter) at pH 5, 6.5 and 8. Right column: B channel (anionic state, excitation at $\lambda_{\text{exc}} = 870\ \text{nm}$ and collection through a 535/30 emission filter) at different pH values (5, 6.5 and 8). Rectangles on the images indicate all single molecules as determined through the histogram analysis. Single proteins present in the A state are not visible in the B state and vice versa. When increasing the pH, the anionic B state (right) is more populated than the neutral A state (left). The ground-state population is: $N(780,440) = 9$, $N(870,525) = 2$ at pH 5, $N(780,440) = 5$, $N(870,525) = 6$ at pH 6.5 and $N(780,440) = 2$, $N(870,525) = 9$ at pH 8. Since in these measurements there is no bleaching, $N(780,440) + N(870,525) = 11$ at all pH values. The single-protein spots correspond to approximately 121 pixels (and $\approx 360\ \mu\text{s}$ acquisition time) on the image and to a total number of counts per spot of 15, 10 and 5 for the pH 5, 6.5 and 8 (neutral state), and 5, 11 and 15 for the anionic state at pH 5, 6.5 and 8. The background on the image is approximately 1 count per 121 pixels area. The spots not included in the rectangles are aggregates of order between four and seven. The left graph shows the number of molecules counted on the two channels, neutral (■) and anionic (○), versus pH on a sample of $N = 88$ total proteins. The error bars indicate the Poisson uncertainty due to the finite number of molecules sampled ($= N^{0.5}$). The right graph shows the free energy change ΔG_j for the reaction $A \rightarrow B + H^+$ measured versus temperature at pH 5. The solid line represents a fit to the van't Hoff equation.

ground level (Figure 3, panel A). Here we call “bleaching” any transition from a fluorescent (A or B) state to a dark state D independent of its origin. The time, $t_{\text{bleaching}}$, at which the bleaching transition occurs, depends on the excitation intensity. The bleached single molecules did not recover spontaneously the

fluorescence emission even when left in the dark for 180–600 s, contrary to what was found for GFP-E222Q mutants^[17] and single dyes.^[28] The distribution of the bleaching time can be fitted to a Gaussian (Figure 3, panel C) for both the electronic transitions. The average value of the bleaching rate, $\Gamma = 1/t_{\text{bleaching}}$, depends on the excitation power as $\Gamma = \gamma_j P_j^{\kappa_j}$, $j = A, B$. The fit of the experimental bleaching rate to this function gives $\kappa_A = \kappa_B = 2.5 \pm 0.3$ and $\gamma_A = 7.7 \times 10^{-3} \pm 2 \times 10^{-3}\ \text{Hz}(\text{mW})^{-2.5}$, $\gamma_B = 1.05 \times 10^{-2} \pm 1 \times 10^{-3}\ \text{Hz}(\text{mW})^{-2.5}$ (Figure 3, panel B).

We also observed fluorescence blinking on the B state only. The duration t_{off} and t_{on} of the “off” and “on” states are in the range of 1–40 ms, depending on the excitation power. The distribution of these times can be described by an exponential behavior (Figure 3, panel D). However, while the average value of $\langle t_{\text{off}} \rangle$ does not change appreciably with the excitation power, the average value of $\langle t_{\text{on}} \rangle$ decreases as P^{-2} (see Figure 3, panel D, inset).

The molecules that fell into the dark state D could recover fluorescence emission after they were illuminated with shorter wavelengths in the range 710–740 nm. These wavelengths are approximately double the value (365 nm) of the absorption peak of a photoreversible, optically inactive configuration observed in bulk solutions of E²GFP.^[32] The recovery efficiency, defined as the ratio of the molecules that recovered fluorescence emission over the total bleached molecules, depends on the excitation power and on the irradiation time. The longer the irradiation time, the higher the number of the molecules that could recover fluorescence emission (Figure 4).

The difference between the single-molecule fluorescence emission before and after the bleaching/recovery cycle is always within the statistical uncertainty due to the shot noise. We collect typically 10–30 photons per sampling time (30–80 kHz fluorescence rate). Within the Poisson uncertainty of 20–30% we do not see a systematic change in the fluorescence output of the single proteins upon fluorescence recovery. The dependence of the recovery efficiency on the wavelength is sharp, with a maximum at 720 nm (inset of Figure 4) where up to 95% of the bleached molecules could recover fluorescence emission. The spectral shape of the fluorescence recovery efficiency does not seem to change appreciably with the excitation power and with the bleached state, A or B (data not shown).

Discussion

According to the results described above, we can propose an energy level diagram for E²GFP (see Figure 5) that includes at least two fluorescent states (A and B) whose population and emission is sensitive to the pH of the environment, and two dark states (Z and D). By comparing the lifetime values and the pH trend of the relative population of the A and B states of the E²GFP with those of other GFP mutants we suggest that the A spectral component corresponds to a neutral state and the B component to an anionic state of the GFP chromophore.^[33] The number of molecules, $N(780,440)$ and $N(870,535)$, on the A and B channels occur in a definite ratio that depends

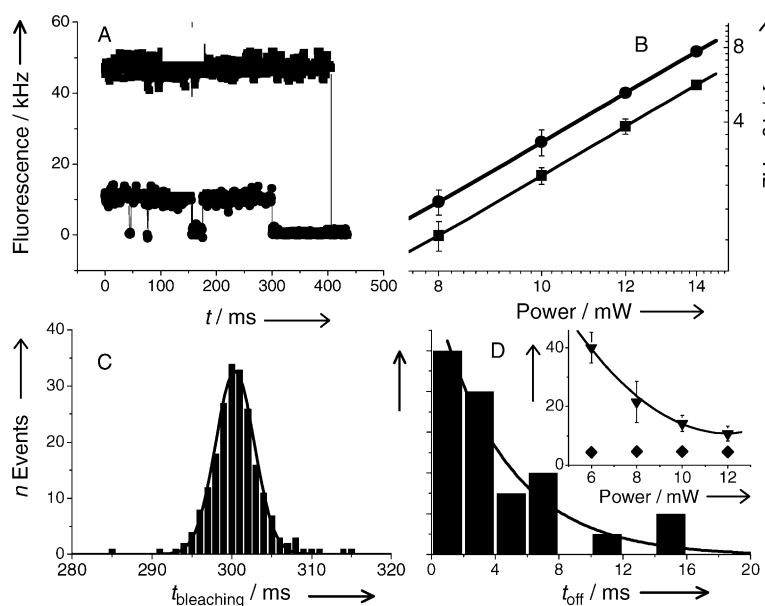


Figure 3. Panel A: typical fluorescence kinetics of single molecules (at pH 5) in the neutral (■) and in the anionic (●) states under 10 mW excitation power versus time. Panel B: bleaching rate $\Gamma = 1/t_{\text{bleaching}}$ averaged over ≈ 100 molecules for the A state (■) with excitation at 780 nm and emission through the 440/50 filter, and for the B state (●) with excitation at 870 nm and emission through the 535/30 filter. Solid lines are the best fit to the function: γP^x . The best-fit values of the parameters are reported in the text. Panel C: histogram of the bleaching time $t_{\text{bleaching}}$ at 10 mW for the anionic state. The solid line is the best-fit Gaussian function to the data. Panel D: histogram of the blinking time t_{off} at 10 mW excitation power. The solid line is a monoexponential fit to the data. Inset of panel D: average values of $\langle t_{\text{on}} \rangle$ (▼) and $\langle t_{\text{off}} \rangle$ (◆) versus the excitation power. The solid line is a $\sim P^{-2}$ best fit to the t_{on} data.

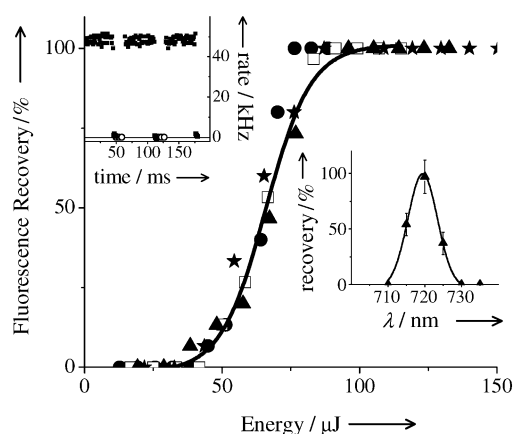


Figure 4. Percentage of the bleached E^2 GFP molecules that recover fluorescence emission after the illumination time at 720 nm for different excitation powers on the sample: 3.3 mW (☆), 4.3 mW (▲), 5 mW (□) and 5.7 mW (●). The data are plotted versus the product of the irradiation time and the irradiation energy at 720 nm, which is proportional to the absorbed energy (see text for a discussion). The solid line is the best fit to a sigmoid function, $y = A_2 + (A_1 - A_2) / [1 + \exp((x - x_0)/dx)]$ with values $A_2 = 100 \pm 1.5$, $A_1 = 0.2 \pm 1.5$, $dx = 8.2 \pm 0.7$ and $x_0 = 66 \pm 0.7 \mu\text{J}$. Right inset: fluorescence recovery efficiency at fixed illumination time (20 ms) and excitation power (4.3 mW) versus the excitation wavelength. The solid line is a best fit to a Gaussian function. Left inset: fluorescence rate collected from a single protein with excitation power = 10 mW (at $\lambda = 780$ nm, pH 5). After each bleaching event, the protein was irradiated for 14 ms at 720 nm with an irradiation power of 5.7 mW. For clarity, we plot one in every five points. Filled squares (■) and open circles (○) indicate the fluorescence emission upon 780 nm excitation and 720 nm irradiation.

on the silica gel pH (Figure 2, left graph) and temperature (Figure 2, right graph). In a first approximation $N(780,440)$ and $N(870,530)$ should be equal to the number of molecules (N_A ,

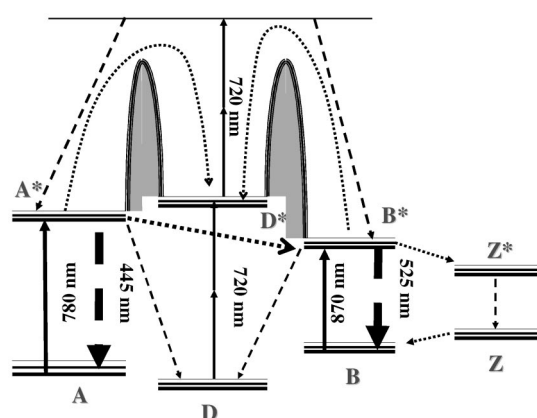


Figure 5. Scheme of the proposed electronic levels structure for E^2 GFP. A is the neutral state, B is the anionic state, Z is the zwitterionic state, D is the dark state. The solid lines indicate the excitation paths, the thick dashed lines indicate the radiative transitions, the thin dashed lines indicate the nonradiative transitions between excited and ground states, and the dotted lines indicate the conversions between excited or ground states ($A^* \rightarrow B^*$, $B^* \rightarrow Z^*$ and $Z \rightarrow B$). The excitation and emission wavelengths are indicated in the graph. The gray areas indicate the energy barriers to be overcome in order to recover fluorescence emission.

N_B) in the ground A and B states, respectively. False assignments of the molecules to the two states could be possible due to the photoconversion between the excited A^* and B^* states that can also be observed in the spectra of Figure 1 (panel D). In fact, a detailed analysis of the TPE and OPE spectra^[34] indicates a photoconversion $A^* \rightarrow B^*$ efficiency $\approx 20\%$, as found for other GFP mutants.^[33] However, due to the difference in brightness of the two states, we estimate that the numbers

$N(780,440)$, $N(870,530)$ reproduce N_A and N_B within the experimental uncertainties. A complete study of a second GFP mutant^[35] and preliminary studies on E²GFP show that low excitation intensities and large image sampling time (the time between one image and the subsequent one) diminish the photoconversion probability. The data reported in Figure 2 are taken with a very large image sampling time (that in this case is the time needed to exchange pH in the gel) and at low excitation power ($P \approx 10$ mW). In this case the photoconversion probability is kept at a minimum, although it cannot be abolished. We can therefore estimate the free energy gap between the anionic and neutral states from the Equation (1):

$$\frac{N(780,440)}{N(870,535)} \simeq \frac{N_A}{N_B} = e^{-\frac{\Delta G}{RT}} \quad (1)$$

The experimental value, obtained by an average over 60 single proteins, $N_A/N_B = 4.4 \pm 1.2$ determined at pH 5, implies that the difference in the free energy between the two states is $G_B - G_A = 3.5 \pm 0.7$ kJ mol⁻¹. We have then determined the enthalpy and entropy change for the deprotonation reaction $A \rightarrow B + H^+$. In this case we have measured the ratio N_B/N_A over a sample of 88 single molecules at pH 5.5 in the temperature range 2 °C to 50 °C, and evaluated the deprotonation equilibrium constant as given in Equation (2):

$$K_{\text{eq}} = \frac{N_B}{N_A} 10^{-\text{pH}} \quad (2)$$

The temperature dependence of the equilibrium constant allows the calculation of the standard reaction enthalpy ΔH_d^0 according to the van't Hoff Equation (3):

$$-\frac{d}{d(1/T)} \ln(K_{\text{eq}}) = \frac{\Delta H_d^0}{R} \quad (3)$$

where R is the gas constant $R = 8.31$ J K⁻¹ mole⁻¹. From the linear fit reported in the right plot of Figure 2 we obtain $\Delta H_d^0 = 3.6 \pm 0.2$ kJ mol⁻¹, and from this a standard entropy change $\Delta S_d^0 = -105 \pm 5$ kJ mol⁻¹ K⁻¹. The trend and the values of the free energies reported here are very similar to those reported by Haupts et al.^[5] for EGFP at pH 6.5.

Theoretical predictions and low temperature measurements^[36] indicate that a fourth metastable state I exists,^[37] which acts as an intermediate between the A* and B* states. This state has recently been stabilized^[38] and observed in a GFP mutant (with mutations Thr203 Val and Glu222Gln). It is suggested that the excited I* state can decay through direct fluorescence to its ground state with fast conversion into the ground A state or through a rapid conversion of I* to the excited B* state.^[37,39] Although we do not observe a third emission band (Figure 1, panel A) in the fluorescent spectrum, we cannot discriminate between these two possible relaxation pathways since the I and B emissions largely overlap.^[39]

The transition of a single E²GFP from the anionic B state to the zwitterionic state can account for the reversible process of blinking. In fact the zwitterionic Z form has been reported to

be a dark state.^[33,40,41] On the other hand the photoconversion between the excited states A* (RH^* in ref. [39]) and B* (R_{neq}^* in ref. [39]), due to a proton transfer process is expected to be slower than ≈ 10 ns.^[37,39] In the ms range, no blinking process is observed for the A state. The distribution of the blinking off- and on-times is well described by an exponential function (Figure 3, panel D) with average values in the order of milliseconds. However, while $\langle t_{\text{off}} \rangle$ does not vary appreciably with the excitation power, the average values of the on-times, $\langle t_{\text{on}} \rangle$, shows a clear quadratic dependence on the excitation power (see Figure 3, panel D, inset). According to Weber et al.,^[41] we assign the blinking off-transition to a conversion between the excited B* and Z* states. Its probability would depend on the B \rightarrow B* excitation and, therefore, on the second power of the excitation intensity. On the other hand, the fact that $\langle t_{\text{off}} \rangle$ does not change with the excitation power suggests that the E²GFP protein may spontaneously relax to the B state, from which the fluorescence cycle can start over again. This would indicate that the ground Z state lies at higher energy than the ground B state and that there is a very low energy barrier to be overcome for this process.

The transition from the A or B state to the dark D state is apparently an irreversible process, which we call bleaching. The approximately second-order power law of the bleaching rate Γ upon the excitation power P (Figure 3, panel B) is expected since bleaching usually occurs from excited states that are reached here by two-photon absorption. Similar findings have been reported from bulk measurements on simple fluorophores on microdroplets by Patterson et al.^[42] However the bleaching time has a Gaussian distribution (Figure 3, panel C) and this is a strong indication that the observed process is not due to a transition from the excited singlet to a dark state, a process that should be characterized by an exponential distribution of bleaching times.^[6]

Our data indicate that, at acidic pH, the A state lies slightly lower than the B state, while the energy level of A* is slightly higher than that of B*. This assignment comes from the measurement of the equilibrium ratio N_A/N_B and from the emission Stokes shifts. Blinking suggests that there is a conversion between the B and Z states both at the ground (t_{off}) and at the excited (t_{on}) states (Figure 5). On the other hand, bleaching is probably related to the transition from the excited states A* and B* to a dark state D* that converts non-radiatively to D. It is not possible from the present study to infer whether the A*–D* transition is more likely to occur than the B*–D* one, since the bleaching times are very similar for the two excitation bands and have similar dependence on the excitation power. The dark D state to which the molecules convert is different from the zwitterionic Z state for which the fast blinking is observed.^[22,36]

The fluorescence emission from single E²GFP molecules that have been bleached by two-photon excitation at 780 or 870 nm, can be recovered upon excitation at 710–730 nm. In particular, we observed that the recovery of the fluorescence has a sharp dependence on the irradiation wavelength with a maximum at 720 nm (see inset Figure 4). Moreover, the fluorescence recovery efficiency depends upon the irradiation time

times the irradiation power. This parameter is proportional to the total energy released to the molecules (Figure 4). The actual released energy could be computed from the knowledge of the two-photon absorption cross section at 720 nm. The recovery efficiency reaches 50% for an energy release of approximately 65 μJ . Furthermore, experiments on the fluorescence recovery of proteins selectively bleached on either the neutral or anionic state^[34] indicate that two separate dark states may be present in E²GFP. The recovery of the fluorescence upon irradiation at ≈ 720 nm suggests that the D–D* transition would correspond to an energy gap much larger than those related to the other transitions of the chromophore (Figure 5) and probably related to the 360-nm absorption band found upon OPE.^[22,32] The observation that the recovery efficiency spectrum is quite sharp around 720 nm (Figure 4) suggests that the distribution of the vibrational levels of the D states is relatively narrow, and/or that the recovery is a combination of more than one excitation step, as also confirmed by the steepness of the dependence of the fluorescence recovery efficiency upon the released energy. Actually the narrowness of the recovery efficiency spectrum (inset of Figure 4) is one of the most attractive features of E²GFP. As a final remark, we notice that the almost complete recovery of the fluorescence upon irradiation at 720 nm, calls for a word of caution about the actual origin of the so-called “dark state”. In fact we would expect that a fraction of the bleached proteins undergo a photo-chemical reaction from D* and could not recover fluorescence at all. The almost 100% fluorescence recovery observed here, suggests that proteins do not undergo an irreversible chemical reaction from the so-called dark state.

Conclusions

Various pathways among the neutral, the anionic B and the dark zwitterionic state of E²GFP have been observed. The characteristic times for the conversions among these states range from \approx one to several milliseconds. Moreover we have observed bleaching of single E²GFP molecules after ≈ 10 ms⁻¹ s of irradiation in the near-infrared (at 780 nm or 870 nm), depending on the excitation power. This process is probably due to a conversion to a fourth dark D state from which the fluorescence can be recovered with very high efficiency only upon irradiation at 720 ± 10 nm. Two striking features are that the recovery of the fluorescence reaches $\approx 100\%$ at 720 nm and that it has a sharp dependence upon the irradiation power and the illumination time. This GFP mutant seems therefore promising as an almost permanent chromophore for TPE microscopy. Moreover E²GFP could be valuable also for applications in single-molecule memory arrays. In fact the possibility to use IR radiation and high spatial resolution of the two-photon excitation process would allow to have high-density three-dimensional single-molecule memories, where the “0” and “1” bits are dark and bright states and the “erase” and “write” instruction are obtained by illumination at 780 nm and 720 nm, respectively. These possibilities will require further characterization and optimization of the E²GFP mutant, which are currently in progress.

Acknowledgements

This research has been funded by PRIN 20030203741 to G.C. and A.D., by FIRB project “Nanonobiotechnology” to G.C. and F.B., by the FISR 2003 project “Nanotechnology and Biosystems” to G.C. and by the Human Frontier Research Program to V.P. We thank Riccardo Nifosi and Valentina Tozzini for useful discussions and Caterina Arcangeli, Mauro Giacca and Arianno Sabò for preparation of the E²GFP mutant.

Keywords: bleaching · blinking · fluorescence spectroscopy · proteins · single-molecule studies

- [1] L. Song, E. J. Hennink, I. T. Young, H. J. Tanke, *Biophys. J.* **1995**, *68*, 2588–2600.
- [2] G. S. Harms, L. Cognet, P. H. M. Lommerse, G. A. Blab, T. Schmidt, *Biophys. J.* **2001**, *80*, 2396–2408.
- [3] W. Denk, D. Piston, W. W. Webb in *Handbook of Confocal Microscopy* (Ed.: J. B. Pawley), Plenum, New York, **1995** pp. 445–457.
- [4] J. Mertz, *Eur. Phys. J. D* **1998**, *3*, 53–66.
- [5] U. Haupts, S. Maiti, P. Schwille, W. W. Webb, *Proc. Natl. Acad. Sci. USA* **1998**, *95*, 13 573–13 578.
- [6] M. F. Garcia-Parajo, G. M. J. Segers-Nolten, J. A. Veerman, J. Greve, N. F. van Hulst, *Proc. Natl. Acad. Sci. USA* **2000**, *97*, 7237–7242.
- [7] R. I. Paramban, R. C. Bugos, W. W. Su, *Biotech. Bioeng.* **2004**, *86*, 687–697.
- [8] A. Miyawaki, T. Nagai, H. Mizuno, *Curr. Opin. Chem. Biol.* **2003**, *7*, 557–562.
- [9] R. Y. Tsien, *Annu. Rev. Biochem.* **1998**, *67*, 509–564.
- [10] K. F. Sullivan, S. A. Kay, *Green Fluorescent Proteins*, Academic, San Diego, **1999**.
- [11] P. Schwille, *Cell Biochem. Biophys.* **2001**, *34*, 383–408.
- [12] R. M. Dickson, A. Cubitt, R. Y. Tsien, W. E. Moerner, *Nature* **1997**, *388*, 355–358.
- [13] A. Zumbusch, G. Jung, *Single Mol.* **2000**, *1*, 261–270.
- [14] J. Lippincott-Schwartz, G. H. Patterson, *Science* **2003**, *300*, 87–91.
- [15] R. A. Cinelli, A. Ferrari, V. Pellegrini, M. Tyagi, M. Giacca, F. Beltram, *Photochem. Photobiol.* **2000**, *71*, 771–6.
- [16] J. Ellenberg, J. Lippincott-Schwartz, J. F. Presley, *Biotechniques* **1998**, *25*, 838–42.
- [17] G. Jung, J. Wiehler, W. Göhde, J. Tittel, T. Basché, B. Steipe, C. Bräuchle, *Bioimaging* **1998**, *6*, 54–61.
- [18] G. Jung, J. Wiehler, B. Steipe, C. Bräuchle, A. Zumbusch, *ChemPhysChem* **2001**, *2*, 392–396.
- [19] G. H. Patterson, J. Lippincott-Schwartz, *Science* **2002**, *297*, 1873–1877.
- [20] R. Ando, H. Hama, M. Yamamoto-Hino, H. Mizuno, A. Miyawaki, *Proc. Natl. Acad. Sci. USA* **2002**, *99*, 12 651–6.
- [21] D. M. Chudakov, V. V. Belousov, A. G. Zaraisky, V. V. Novoselov, D. B. Staroverov, D. B. Zorov, S. Lukyanov, K. A. Lukyanov, *Nat. Biotechnol.* **2003**, *21*, 191–4.
- [22] R. A. G. Cinelli, V. Pellegrini, A. Ferrari, P. Faraci, R. Nifosi, M. Tyagi, M. Giacca, F. Beltram, *Appl. Phys. Lett.* **2001**, *79*, 3353–3355.
- [23] A. Esposito, F. Federici, C. Usai, F. Cannone, G. Chirico, M. Collini, A. Diaspro, *Micr. Res. Tech.* **2004**, *63*, 12–17.
- [24] A. Diaspro, M. Corosu, P. Ramoino, M. Robello, *IEEE Eng. Med. Biol.* **1999**, *30*, 18–22.
- [25] A. Mozzarelli, S. Bettati in *Advanced Functional Molecules and Polymers, Vol. 4: Functional Properties of Immobilized Proteins* (Ed.: H. S. Nalwa), Gordon and Breach Science Publisher, Singapore, **2001**, pp. 55–97.
- [26] G. Chirico, F. Cannone, S. Beretta, A. Diaspro, B. Campanini, S. Bettati, R. Ruotolo, A. Mozzarelli, *Protein Sci.* **2002**, *11*, 1152–1161.
- [27] G. Chirico, F. Cannone, S. Beretta, G. Baldini, A. Diaspro, *Microsc. Res. Tech.* **2001**, *55*, 359–364.
- [28] G. Chirico, F. Cannone, G. Baldini, A. Diaspro, *Biophys. J.* **2003**, *84*, 588–598.
- [29] A. Volkmer, V. Subramaniam, D. J. S. Birch, T. M. Jovin, *Biophys. J.* **2000**, *78*, 1589–1598.

- [30] G. T. Hanson, T. B. McAnaney, E. S. Park, M. E. P. Rendell, D. K. Yarbrough, S. Chu, L. Xi, S. G. Boxer, M. H. Montrose, S. J. Remington. *Biochem.* **2002**, *41*, 15477–15488.
- [31] T. N. McAnaney, E. S. Park, G. T. Hanson, S. J. Remington, S. G. Boxer. *Biochem.* **2002**, *41*, 15489–15494.
- [32] R. Nifosi, A. Ferrari, C. Arcangeli, V. Tozzini, V. Pellegrini, F. Beltram, *J. Phys. Chem. B* **2003**, *107*, 1679–1684.
- [33] T. M. H. Creemers, A. J. Lock, V. Subramaniam, T. M. Jovin, S. Völker, *Nature Struct. Biol.* **1999**, *6*, 557–560.
- [34] G. Chirico, A. Diaspro, F. Cannone, C. Arcangeli, S. Bologna, V. Pellegrini, F. Beltram, *Phys. Rev. E* in press, **2004**, 70, 030901R(1–h).
- [35] G. Chirico, F. Cannone, A. Diaspro, G. Baldini, **2004**, unpublished results.
- [36] T. M. H. Creemers, A. J. Lock, V. Subramaniam, T. M. Jovin, S. Voelker, *Proc. Natl. Acad. Sci. USA* **2000**, *97*, 2974–2978.
- [37] M. Chatteraj, B. A. King, G. U. Bublitz, S. G. Boxer, *Proc. Natl. Acad. Sci. USA* **1996**, *93*, 8362–8367
- [38] J. Wiehler, G. Jung, C. Seebacher, Z. Zumbusch, B. Steipe, *ChemBioChem* **2003**, *4*, 1164–1171.
- [39] H. Lossau, A. Kummer, R. Heinecke, F. Pollinger-Dammer, C. Kompa, G. Bieser, T. Jonsson, C. M. Silva, M. M. Yang, D. C. Youvan, M. E. Michel-Beyerle, *Chem. Phys.* **1996**, *213*, 1–16.
- [40] P. Schwille, S. Kummer, A. A. Heikal, W. E. Moerner, W. W. Webb, *Proc. Natl. Acad. Sci. USA* **2000**, *97*, 151–156.
- [41] W. Weber, V. Helms, J. A. McCammon, P. W. Langhoff, *Proc. Natl. Acad. Sci. USA* **1999**, *96*, 6177–6182
- [42] G. H. Patterson, D. W. Piston. *Biophys. J.* **2000**, *78*, 2159–2162.

Received: July 8, 2004

Revised: November 11, 2004